Progress In Electromagnetics Research M, Vol. 46, 113–123, 2016

Hybrid Excited Vernier Machines with All Excitation Sources on the Stator for Electric Vehicles

Liang Xu, Guohai Liu, Wenxiang Zhao*, and Jinghua Ji

Abstract—In this paper, two new hybrid excited vernier machines with surface and interior V-shaped PM arrays are proposed. By integrating the vernier structure and field excitation windings together, the proposed machines not only retain the merit of high torque of permanent magnet vernier, but also offer flexible flux adjustment to enable a wide speed range with the introduction of field windings. Different from existing hybrid excited vernier machines having magnets on the rotor, the proposed machines is designed with all excitation sources on the stator. Therefore, temperature rise of magnets of the proposed machines is much easier to control, which in turn reduce the risk of irreversible demagnetization of magnets and enhance the reliability. The electromagnetic performances of the two proposed machines are comprehensively analyzed and quantitatively compared by using the time-stepping finite-element method, verifying the theoretical analysis.

1. INTRODUCTION

Due to the increasing fossil prices and environmental pollution rises, electric vehicles are attracting more and more attention nowadays. The demand for high performance electric machine, as an essential component in electric vehicles, is urgent, especially the one with high power, high efficiency and high reliability [1–5]. The permanent magnet (PM) vernier (PMV) machine developed from the magnetic gears is regarded as an excellent solution for electric vehicles [6–13]. This is because the PMV machine not only retains the merit of high torque of the magnetic gear, but also possesses a simpler mechanical structure with only one air-gap [12–16].

On the other hand, similar to conventional PM machine, the PM magnetic field of PMV machine is difficult to regulate, which leads to limited speed range [17–21]. In order to solve the problem, new kinds of variable flux PM machines were investigated and presented, where except for the armature windings and magnets, they employed either field excitation windings or AlNiCo PMs to facilitate the flux adjustment [17–21]. For the PMV machines, their variable flux counterparts, hybrid excited vernier machine with field excitation windings and memory PMV machine with AlNiCo PMs were proposed in [19] and [21], respectively. Obviously, these machines can offer excellent flux adjustment capability due to their additional excitations. Meanwhile, it is noticed that the hybrid excited vernier machine takes the advantages of a simpler mechanical structure, more convenient flux adjustment and reduced manufacturing cost due to the absence of the AlNiCo PMs in comparison with the memory counterpart, which is very desirable for the electric vehicle applications. Nevertheless, the hybrid excited vernier machine presented in [19] also suffered from drawbacks of low adjusting flux efficiency. It is because the adoption of surface mounted PM array in the existing machine results in relatively high air gap magnetic reluctance, which significantly reduces magnetic fluxes produced by field winding current. As well known, the machines for electric vehicle applications have high power density. Consequently, the

Received 3 December 2015, Accepted 11 January 2016, Scheduled 29 January 2016

* Corresponding author: Wenxiang Zhao (zwx@ujs.edu.cn).

The authors are with the School of Electrical and Information Engineering, Jiangsu University, No. 301 Xuefu Road, Zhenjiang 212013, China.

temperature rises of the machines are high due to their high power losses and small machine size. To ensure the safety of the electric vehicle, the temperature rise of the machines must be well managed. However, the PMs of the existing machine are on the rotor and rotate with the rotor, and thermal management for PMs of the existing machine is more difficult than that of the stator-PM machines presented in [22]. Consequently, the possibility of irreversible demagnetization of PMs of the existing machine is increased due to its difficult thermal management for PMs, which reduces the reliability of the existing machine and limits its potential to be applied into electric vehicles. On the other hand, the controllable flux of the existing hybrid excited vernier machines is only verified at no-load operation, whereas its on-load operation has not been reported.

To solve these problems in the existing hybrid excited vernier machine, two hybrid excited vernier machines with PMs located on the stator will be proposed in this paper. Similar to stator-PM machines presented in [22], the proposed machines having PMs on the stator offer enhanced reliability and simple thermal management for PMs. In Section 2, topology and operation principle of the proposed machines will be introduced. In Section 3, their electromagnetic performances will be analyzed and compared. Finally, conclusions will be drawn in Section 4.

2. TOPOLOGY AND OPERATION PRINCIPLE

The topologies and winding connections of the two proposed three-phase hybrid excited vernier machines are shown in Figure 1 and Figure 2. Both machines have a simple and compact outer rotor structure without PMs and windings. Therefore, the outer rotor can be directly coupled with the rim of the wheel in electric vehicles, offering high dynamic response, space utilization and transmission efficiency. Meanwhile, as the PMs of the both machines are placed in their stator, the management of heat dissipation for PMs is convenient, and the risk of irreversible demagnetization of PMs due to thermal instability can be significantly reduced. Moreover, the surface and V-shaped interior PMs are adopted in the two machines. According to different arrangements for PMs, the proposed machines are termed as hybrid excited surface PMV machine (HE-SPMVM) and hybrid excited V-shaped interior PMV machine (HE-VIPMVM), respectively.

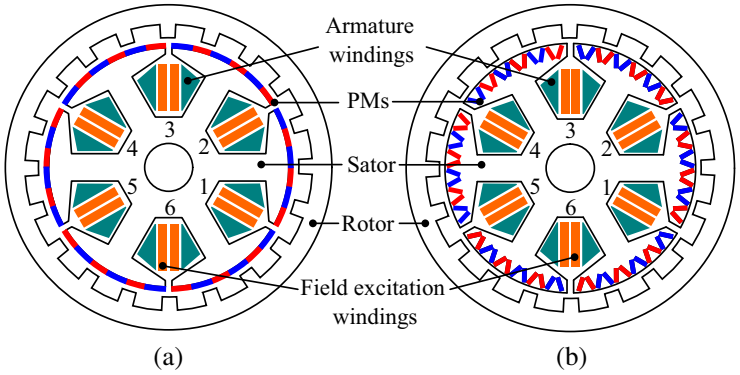

Figure 1. Proposed machines. (a) HE-SPMVM. (b) HE-VIPMVM.

Although the proposed hybrid excited vernier machines introduce additional field windings, they still operate based on flux modulation effect as with the magnetic gears and PMV machines. For the proposed machines, their salient poles in the rotor, which resembles the ferromagnetic segments of the modulation ring in the magnetic gears, can modulate the high speed rotating magnetic field of armature windings to match the low speed rotating magnetic field of PM, hence resulting in high torque and low speed [6]. Similar to the conventional PMV machines, the proposed hybrid excited vernier machines should satisfy the following relationships [6]:

$$p_w = |N_r - p_s| \tag{1}$$

where N_r is the number of salient poles on the rotor, p_w the pole-pairs number of the armature windings, and p_s the pole-pairs number of the PM in the stator. In addition, the corresponding gearing ratio G_r

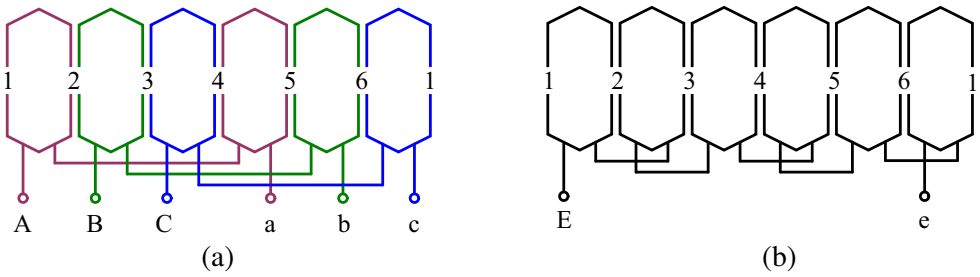

Figure 2. Winding connections. (a) Armature windings. (b) Field excitation windings.

is given by

$$G_r = \frac{N_r}{p_w} \tag{2}$$

There exist many applicable combinations of rotor salient poles and stator winding pole-pairs for the PMV machines. For simplified comparison of the PMV machines with various combinations, the PM pole-pairs of the proposed machines are set to a constant of 18. Then, appropriate combinations for the proposed machines are listed in Table 1. As revealed in [10], the PMV machines with high gear ratio can offer high torque due to high flux change ratio. Also, it should be noted that different rotor pole-pairs have significant effect on their cogging torques except electromagnetic torques. However, considering the purpose of obtaining the maximum output torque, the candidate with the highest gear ratio is chosen. From Table 1, it can be seen that the proposed machine having 20 rotor pole-pairs possesses the highest gear ratio of 10. Thus, $p_w = 2$, $p_s = 18$, and $N_r = 20$ are chosen for further analysis, in which G_r is 10, indicating that the rotor speed is only 1/10 of that of magnetic field of armature windings, and high torque at low speed can be achieved.

Table 1. Comparison of proposed machines having different rotor salient poles.

Rotor salient poles, N_r	22	20	16	14
PM pole-pairs, p_s	18	18	18	18
Stator winding pole-pairs, p_w	4	2	2	4
Winding factor, k_w	0.866	0.866	0.866	0.866
Gear ratio, G_r	5.5	10	8	3.5

On the other hand, for the conventional PMV machines, their speed ranges are limited because the inverter with limited capacity cannot supply adequate terminal voltage when machines run at a high rotational speed. On the other hand, for the proposed hybrid excited vernier machines, the introduction of field windings can significantly alleviate this problem. By applying appropriate current into the field windings, the air-gap flux density can be easily adjusted for maintaining an appropriate terminal voltage, hence allowing the proposed machines operating at a high speed. Moreover, except for the adjustment for terminal voltage, the electromagnetic torque can be regulated by the field windings. The electromagnetic torque T_e of the proposed hybrid excited vernier machines consists of three components, i.e., PM torque T_{pm}, reluctance torque T_r and field windings torque T_f, which can be expressed as:

$$T_e = T_{pm} + T_r + T_f = \frac{\partial \psi_{pm}^T i}{\partial \theta} + \frac{1}{2}\frac{\partial \left(i^T L i\right)}{\partial \theta} + \frac{\partial \psi_f^T i}{\partial \theta} \tag{3}$$

where T_r of the hybrid excited vernier machines can be ignored owing to the fact that their inductance variations are negligible, and L is the winding inductance, i the armature winding current, ψ_f the flux linkage due to field winding excitation, ψ_{pm} the flux linkage due to PMs and θ the rotor position. Also, from Eq. (3), an additional T_f can be obtained when applying a dc current into the field windings.

Therefore, the hybrid excited vernier machines can run at two modes. One mode is that the hybrid excited vernier machines run at high torque and low speed without applying dc currents into field windings. The other mode is that the hybrid excited vernier machines run at low torque and high speed conditions, in which the field windings are fed by a dc current to weaken the air-gap flux density and flux linkage. Hence, the hybrid excited vernier machines can incorporate the merits of a high torque and a wide speed range.

3. PERFORMANCE ANALYSIS AND COMPARISON

In this section, the electromagnetic performances of the proposed hybrid excited vernier machines are analyzed and compared by using the finite-element (FE) method with Ansys maxwell-2D transient solver. For a fair comparison, they are designed based on identical overall size, air-gap length, gearing ratio and turn numbers per phase. Their main design parameters are listed in Table 2.

As the proposed hybrid excited vernier machines belong to doubly salient PM machines, their cogging torques are relatively large and hence leading to large torque ripple, vibration and noise. As revealed in [16], since the rotor tooth of the PMV machines is utilized as flux modulation poles to regulate the magnetic field, its dimension has great influences on back electromotive force (back-EMF) and cogging torque of the PMV machine. Compared with rotor tooth tip arc, the rotor tooth root arc

Table 2. Main design specifications of proposed machines.

Items	HE-SPMVM	HE-VIPMVM
Rated speed (r/min)	200	200
Number of phases	3	3
Rotor outer diameter (mm)	246	246
Air-gap length (mm)	0.6	0.6
Stack length (mm)	80	80
Number of rotor slots	20	20
Number of PM pole-pairs	18	18
Number of armature winding pole-pairs	2	2
Total magnet volume (cm^3)	114.48	144
Magnet remanence (T)	1.23	1.23
Magnet relative recoil permeability	1.1	1.1

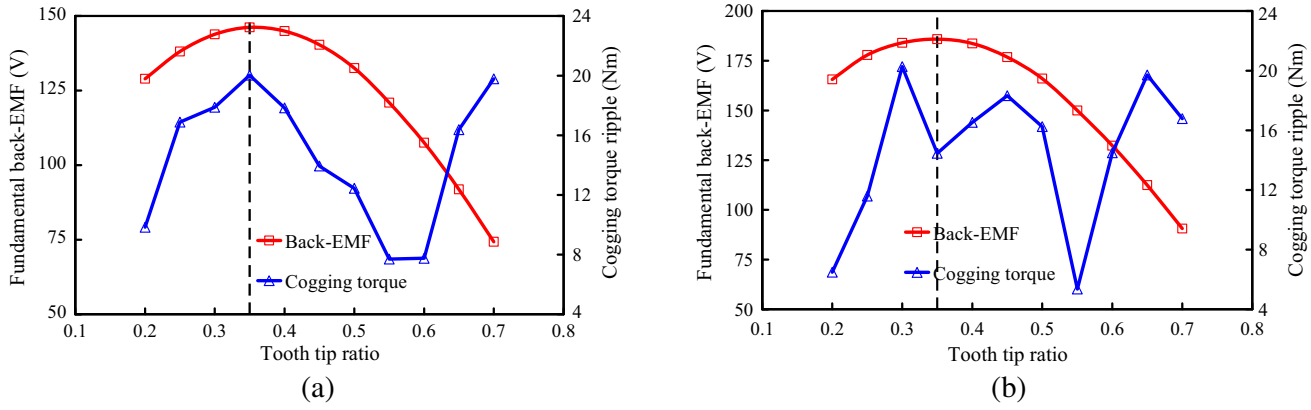

Figure 3. Variations of fundamental back-EMF and cogging torque with tooth tip ratio. (a) HE-SPMVM. (b) HE-VIPMVM.

of the PMV machine has only a slight influence on back-EMF and cogging torque. Hence, the tooth root arc is not considered during the optimization process, and is set to be a relatively large value to avoid the tooth being highly saturated.

Figure 3 depicts the influences of tooth tip ratios of both machines on their back-EMFs and cogging torques, in which the tooth tip ratio denotes the ratio of tooth tip arc to tooth pole pitch. It can be seen that both machines reach their maximum back-EMFs when tooth tip ratio is equal to 0.35, while the cogging torques of the proposed HE-SPMVM and HE-VIPMVM are close to 15 Nm and 20 Nm, respectively, which significantly deteriorate their electromagnetic torque performances. It can be found that the lowest cogging torque of both machines is higher than 5 Nm at the full range of tooth tip ratio. Additionally, in the case of minimum cogging torque, the fundamental back-EMFs of HE-SPMVM and HE-VIPMVM are only about 82% and 81% of their maximum back-EMFs, which significantly reduce their back-EMFs and hence cutting down their electromagnetic torques. Hence, the optimizations of tooth tip ratio are not very effective for minimizing the cogging torques of both machines.

To improve these problems, the rotor skewing technique combined with tooth tip ratio optimization method is employed in this study. The optimizations of rotor skewing degrees of both machines are carried out when the rotor tooth tip ratio is set to 0.35. To evaluate the influence of rotor skewing on the performance, 3-D FE method should be employed, which inevitably consumes an enormous amount of time. In order to avoid 3-D FE method and save calculation time, a multi-step 2-D FE method reported in [23] is used to calculate the performance of proposed machines with skewed rotor.

Figure 4 shows the variations of fundamental back-EMF and cogging torque of both machines versus various skew degrees. It can be seen that the optimal skew degrees of the proposed HE-SPMVM and HE-VIPMVM are 6 and 3 mechanical degrees, respectively. Figures 5 and 6 illustrate their cogging torque and back-EMF waveforms of both proposed machines with skewed rotor and unskewed rotor. As will be seen, the cogging torques of both machines are significantly reduced with skewed rotors, which are much lower than their achievable minimum in the case of tooth tip ratio optimization shown in Figure 3. The results of tooth tip ratio optimization and combined optimization (both skewing rotor and tooth tip ratio optimizations) of the two machines are summarized and compared in Tables 3 and 4. Clearly, it can be seen that the combined optimization method is more beneficial to improving the back-EMF and reducing cogging torque of both proposed machines compared with the tooth tip ratio optimization method. Figures 7 and 8 illustrate the no-load magnetic field distributions of both machines with and without additional field winding excitations. It can be found that both machines form a 4-pole magnetic distributions, implying the effectiveness of the flux modulation effect. Further observation reveals that most of PM fluxes of the HE-VIPMVM can go through corresponding stator teeth due to the flux concentration of V-shaped PM arrangement. This implies that the HE-VIPMVM can offer higher no-load Back-EMF than the HE-SPMVM as shown in Figure 8. Meanwhile, it can be observed that fluxes in some stator teeth of both machines are effectively weakened when their field windings are excited.

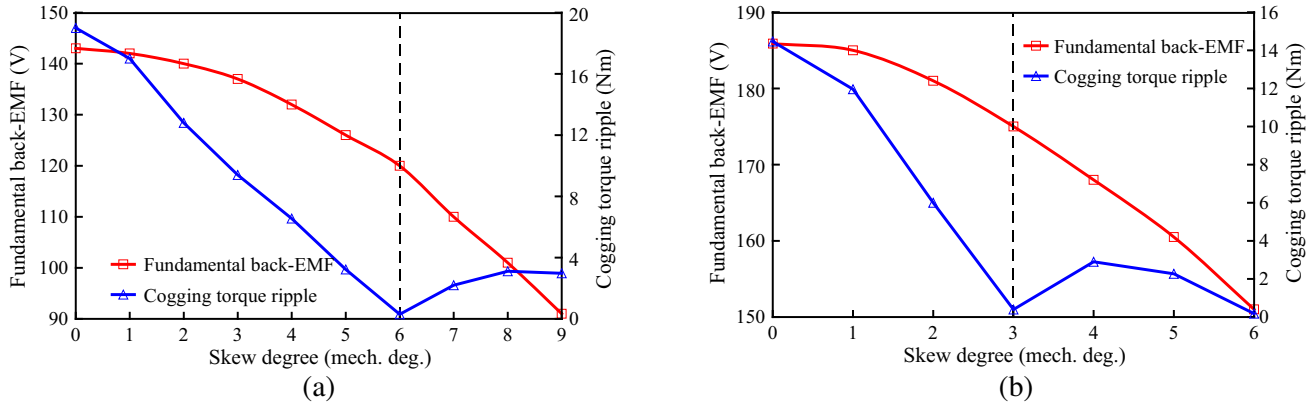

Figure 4. Variations of fundamental back-EMF and cogging torque with different skew degrees. (a) HE-SPMVM. (b) HE-VIPMVM.

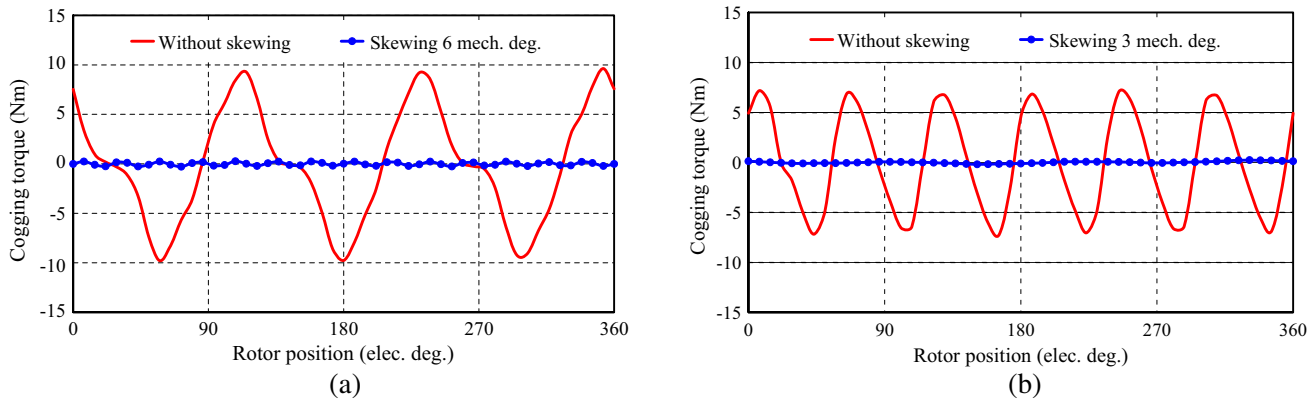

Figure 5. Cogging torques. (a) HE-SPMVM. (b) HE-VIPMVM.

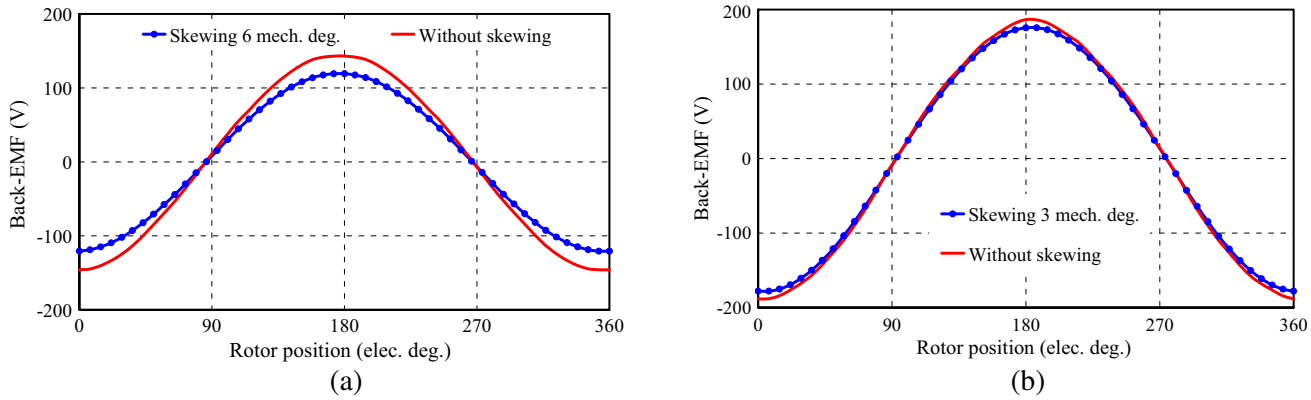

Figure 6. No-load back-EMFs only by PMs. (a) HE-SPMVM. (b) HE-VIPMVM.

Table 3. Optimization results of proposed HE-SPMVM.

Items	Tooth tip ratio optimization	Combined optimization
Tooth tip ratio	0.55	0.35
Rotor skewing degree	0	6
Cogging torque (Nm)	7.7	0.3
Fundamental back-EMF (V)	121	120

Table 4. Optimization results of proposed HE-VIPMVM.

Items	Tooth tip ratio optimization	Combined optimization
Tooth tip ratio	0.55	0.35
Rotor skewing degree	0	6
Cogging torque (Nm)	5.4	0.4
Fundamental back-EMF (V)	150	175

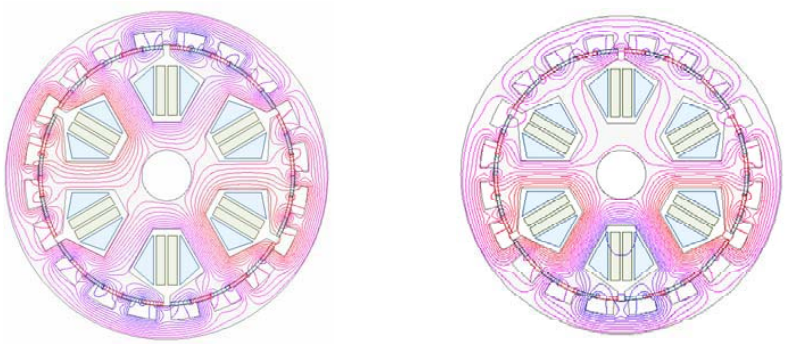

Figure 7. No-load magnetic field distributions of the HE-SPMVM. (a) PMs excitation only. (b) PMs and field winding excitations.

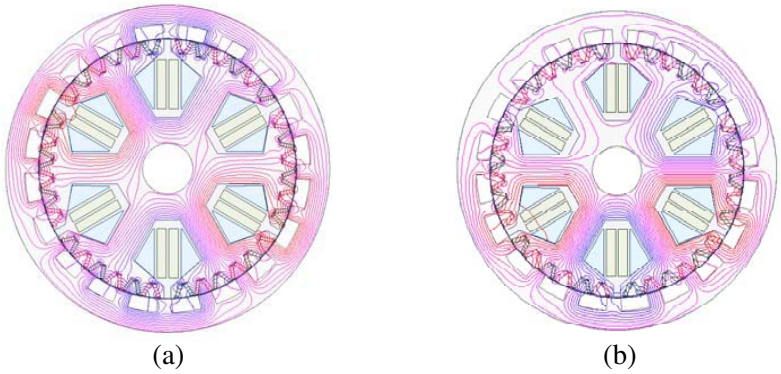

Figure 8. No-load magnetic field distributions of the HE-VIPMVM. (a) PMs excitation only. (b) PMs and field winding excitations.

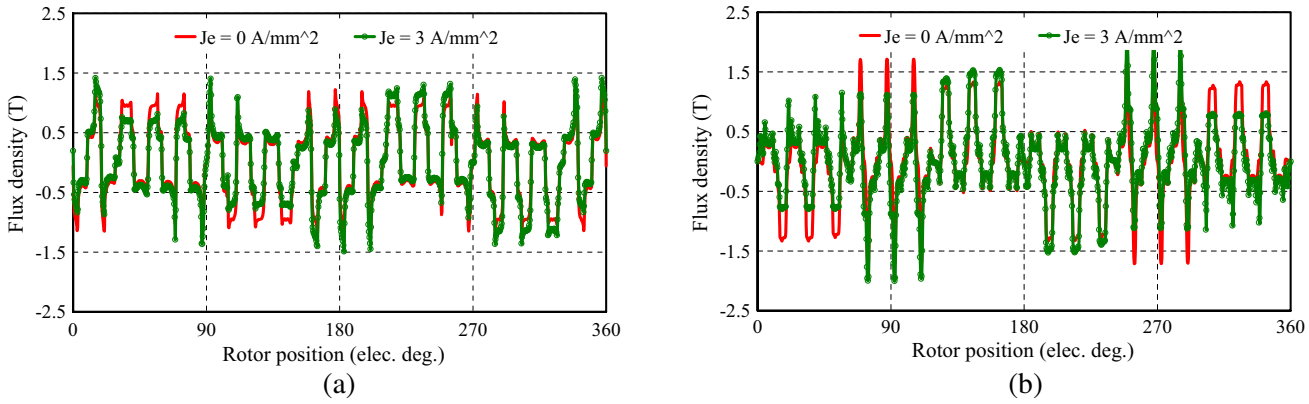

Figure 9. No-load air-gap flux densities. (a) HE-SPMVM. (b) HE-VIPMVM.

Figures 9 and 10 compare the air-gap flux density and corresponding harmonic spectra of both machines with and without field winding excitations. As shown in Figure 9, the air-gap flux densities of both machines are weakened and enhanced at different rotor positions when the additional dc currents are fed into the field windings. However, it should be noticed that the weakening effect for air-gap flux densities is much stronger than the enhancing effect for air-gap flux densities, implying that the air-gap flux densities of both machines can be effectively weakened. Meanwhile, from Figure 10, it can be seen that the 2nd harmonics of air-gap flux densities of both machines, which are the major

components for generating back-EMF and contributing continuous torques, are effectively decreased when additional field windings are supplied with dc currents. The 2nd harmonic component of air-gap flux density of the proposed HE-SPMVM is reduced from 0.23 T to 0.21 T, namely, the reduction is about 8.7%. Also, for the proposed HE-VIPMVM, its 2nd harmonic component of air-gap flux density is reduced from 0.25 T to 0.16 T, namely, the reduction is about 36%, which reveals that the proposed HE-VIPMVM possesses higher flux weakening capability than that of the proposed HE-SPMVM. The higher flux weakening capability of HE-VIPMVM results from its interior PM array type reduces the air gap magnetic reluctance and hence increasing the magnetic fluxes created by the field winding current.

Figure 11 shows the back-EMFs of both machines at rated rotational speed of 200 r/min. It can be seen that their back-EMFs can be regulated with various field windings currents, verifying the effectiveness of the flux controllable ability. Also, it can be found that the HE-VIPMVM can offer higher back-EMF amplitude by 45% and stronger flux adjustment than HE-SPMVM. Figure 12 shows the output torques of both machines with various field windings current densities (Je) when the armature current density is set to 2 A/mm^2. It can be found that the average torques of the HE-SPMVM and HE-VIPMVM without field winding excitation, i.e., $Je = 0$ A/mm^2, are 62.9 Nm and 48.6 Nm, respectively. Namely, the average torque of HE-VIPMVM is 29% higher than that of HE-SPMVM, indicating that the HE-VIPMVM possesses higher torque compared with the HE-SPMVM. However, it should be noticed that the increase of average torque of the HE-VIPMVM is less than that of back-EMF. This is because the magnetic field in HE-VIPMVM is more saturated due to the concentration effect of the V-shaped PM arrangement.

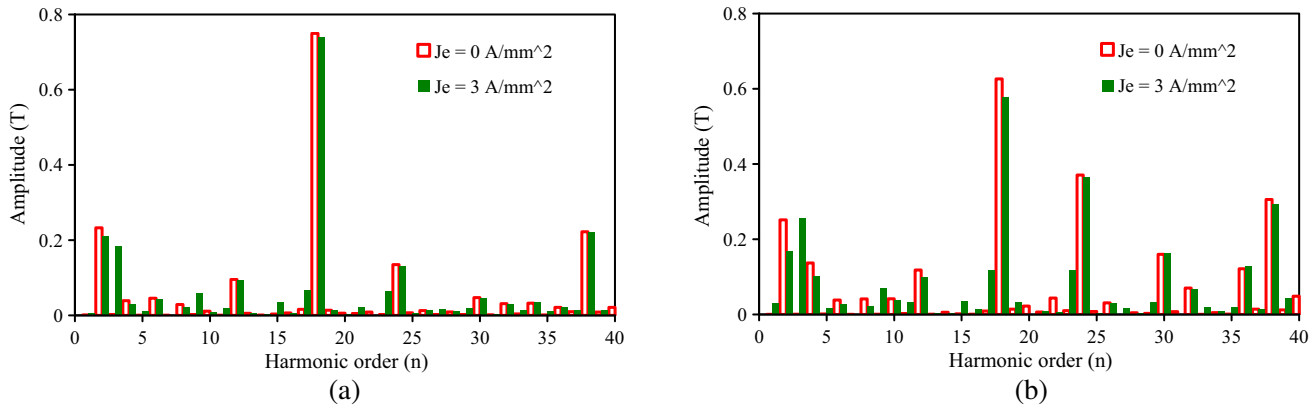

Figure 10. Corresponding harmonic spectra of air-gap flux densities. (a) HE-SPMVM. (b) HE-VIPMVM.

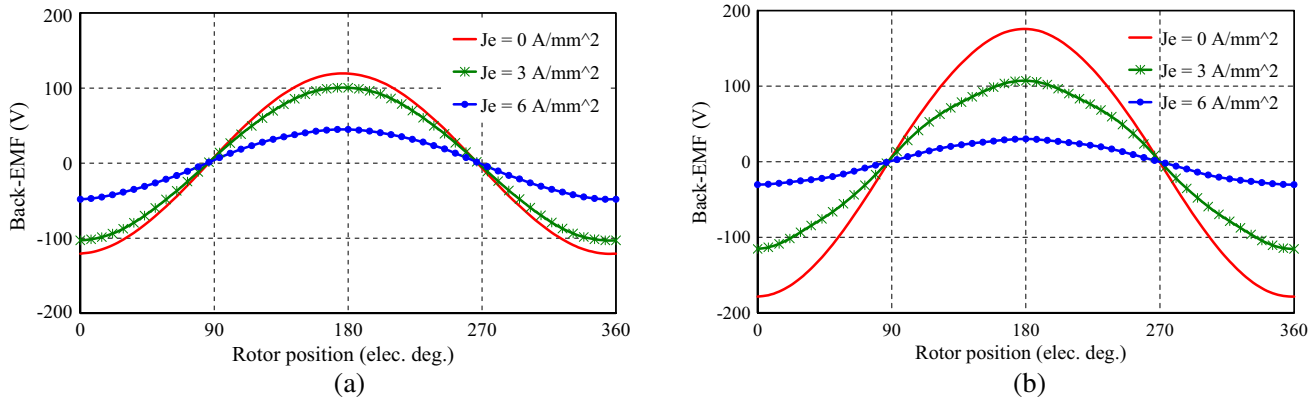

Figure 11. Back-EMF waveforms with various field winding excitations. (a) HE-SPMVM. (b) HE-VIPMVM.

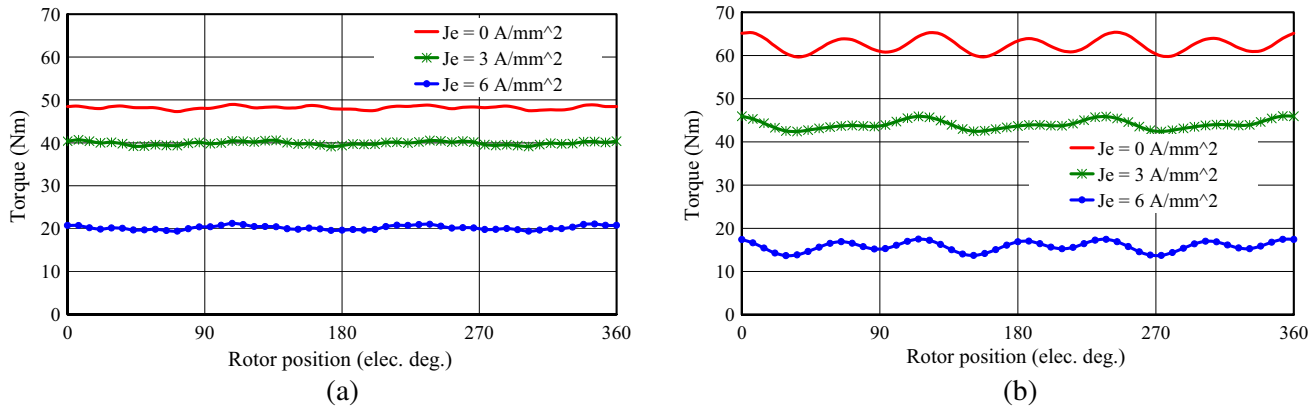

Figure 12. Torque waveforms with various field winding excitations. (a) HE-SPMVM. (b) HE-VIPMVM.

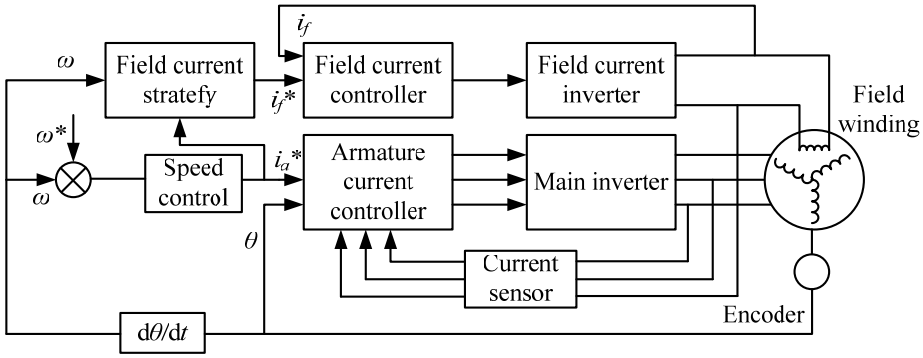

Figure 13. Block-diagram of the drive control system of proposed machines.

Figure 13 illustrates a block diagram of the drive control system of both proposed machines. Differing from conventional PM machines, the proposed machines have the additional field excitation windings. Therefore, in addition to the armature current controller and corresponding inverter, both proposed machines require a field current controller and corresponding inverter, which results in that the control systems of the proposed machines become more complex. Moreover, the additional field excitation windings inevitably cause additional copper losses and hence reducing efficiency when field excitation windings are excited. However, the proposed machines can offer desirable flux weakening capability, extended speed range and flexible flux adjustment. Meanwhile, with appropriate control of the field excitation and armature currents, the total losses and efficiencies of the proposed machines can be reduced and improved.

Figure 14 shows the torque versus speed envelopes of both proposed machines with and without field winding excitations, in which $i_d = 0$ is adopted. Voltage limits of both machines are reached when their rotational speeds are up to their rated speed of 200 r/min. As shown in Figure 14, with the increase of speed, torques of both machines significantly decrease for maintaining the terminal voltage not to exceed their limits, when field windings are not excited. Thus, both machines suffer from very limited operation ranges due to the uncontrollable PM magnetic field. On the other hand, by utilizing the field excitation windings, the magnetic field and flux linkage of both machines can be flexibly weakened to ensure the terminal voltage not to exceed their voltage limits when they operate at high speeds. Hence, the proposed hybrid excited vernier machines take the advantages of flux adjustment ability and wide speed range, as shown in Figure 14. Also, it can be found that the HE-VIPMVM possesses a wider speed range than that of the HE-SPMVM, which is consistent with the results in Figure 11.

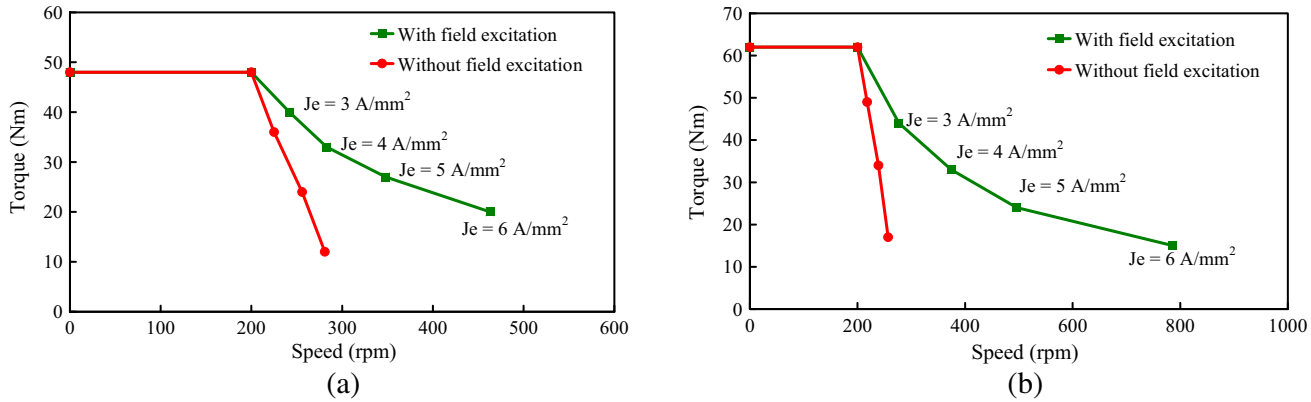

Figure 14. Torque versus speed envelope with and without field winding excitations. (a) HE-SPMVM. (b) HE-VIPMVM.

4. CONCLUSIONS

In this paper, two new hybrid excited vernier machines, namely the HE-SPMVM and HE-VIPMVM, have been proposed, which integrate the merit of a high torque at low speed of PMV machines and the merit of a wide speed range of hybrid excited machines. Moreover, since the PMs and windings of the proposed machines are located in their stator, the heat management for PMs is more convenient than the existing hybrid excited vernier machine with PMs located on the rotor. Therefore, the problems of poor mechanical integrity and thermal instability in the existing hybrid excited vernier machine are solved. Quantitative comparisons between both proposed machines reveal that the HE-VIPMVM can offer higher torque, wider speed range and stronger flux adjustment capability than the HE-SPMVM. However, it is worth mentioning that it also cost much PM material which is about 26% higher than that of the HE-SPMVM. The results verify that both proposed hybrid excited vernier machines have a promising future for high torque and wide speed range applications such as electric vehicles.

ACKNOWLEDGMENT

This work was supported by the National Natural Science Foundation of China (61273154 and 51577084), the Research Fund for 333 Project of Jiangsu Province (Project BRA2015302), the Key Project of Natural Science Foundation of Jiangsu Higher Education Institutions (15KJA470002), the Graduate Education Innovation Project of Jiangsu Province (KYLX-1049), and the Priority Academic Program Development of Jiangsu Higher Education Institutions.

REFERENCES

1. Chau, K.-T., W. Li, and C. H. T. Lee, "Challenges and opportunities of electric machines for renewable energy," *Progress In Electromagnetics Research B*, Vol. 42, 45–74, 2012.
2. Zhu, Z. Q. and D. Howe, "Electrical machines and drives for electric, hybrid, fuel cell vehicles," *Proceeding of IEEE*, Vol. 95, No. 4, 746–765, 2007.
3. Chau, K. T., C. C. Chan, and C. Liu, "Overview of permanent-magnet brushless drives for electric and hybrid electric vehicles," *IEEE Transactions on Industrial Electronics*, Vol. 55, No. 6, 2246–2257, 2008.
4. Liu, G., M. Shao, W. Zhao, J. Ji, Q. Chen, and Q. Feng, "Modeling and analysis of halbach magnetized permanent-magnets machine by using lumped parameter magnetic circuit method," *Progress In Electromagnetics Research M*, Vol. 41, 177–188, 2015.

5. Dorrell, D. G., A. M. Knight, L. Evans, and M. Popescu, "Analysis and design techniques applied to hybrid vehicle drive machines — Assessment of alternative IPM and induction motor topologies," *IEEE Transactions on Industrial Electronics*, Vol. 59, No. 10, 3690–3699, 2012.
6. Toba, A. and T. A. Lipo, "Generic torque-maximizing design methodology of surface permanent-magnet vernier machine," *IEEE Transactions on Industry Applications*, Vol. 36, No. 6, 1539–1546, 2000.
7. Liu, G., J. Yang, W. Zhao, J. Ji, Q. Chen, and W. Gong, "Design and analysis of a new fault-tolerant permanent-magnet vernier machine for electric vehicles," *IEEE Transactions on Magnetics*, Vol. 48, No. 11, 4176–4179, 2012.
8. Li, X., K. T. Chau, M. Cheng, B. Kim, and R. D. Lorenz, "Performance analysis of a flux-concentrating field-modulated permanent-magnet machine for direct-drive applications," *IEEE Transactions on Magnetics*, Vol. 51, No. 5, 1–11, 2015.
9. Li, J., K. T. Chau, J. Z. Jiang, C. Liu, and W. Li, "A new efficient permanent-magnet vernier machine for wind power generation," *IEEE Transactions on Magnetics*, Vol. 45, No. 6, 1475–1478, 2010.
10. Xu, L., G. Liu, W. Zhao, J. Ji, H. Zhou, W. Zhao, and T. Jiang, "Quantitative comparison of integral and fractional slot permanent magnet vernier motors," *IEEE Transactions on Energy Conversion*, Vol. 30, No. 4, 1483–1495, 2015.
11. Jian, L., J. Liang, Y. Shi, and G. Xu, "A novel double-winding permanent magnet flux modulated machine for stand-alone wind power generation," *Progress In Electromagnetics Research*, Vol. 142, 275–289, 2013.
12. Liu, C. and K.-T. Chau, "Electromagnetic design and analysis of double-rotor flux-modulated permanent-magnet machines," *Progress In Electromagnetics Research*, Vol. 131, 81–97, 2012.
13. Li, D., R. Qu, and T. A. Lipo, "High power factor vernier permanent magnet machines," *IEEE Transactions on Industry Applications*, Vol. 50, No. 6, 3664–3674, 2014.
14. Jian, L. and K. T. Chau, "A coaxial magnetic gear with Halbach permanent-magnet arrays," *IEEE Transactions on Energy Conversion*, Vol. 25, No. 2, 319–328, 2010.
15. Li, X., K.-T. Chau, M. Cheng, and W. Hua, "Comparison of magnetic-geared permanent-magnet machines," *Progress In Electromagnetics Research*, Vol. 133, 177–198, 2013.
16. Du, Y., K. T. Chau, M. Cheng, Y. Fan, Y. Wang, W. Hua, and Z. Wang, "Design and analysis of linear stator permanent magnet vernier machines," *IEEE Transaction on Magnetics*, Vol. 47, No. 10, 4219–4222, 2011.
17. Gaussens, B., E. Hoang, M. Lécrivain, P. Manfe, and M. Gabsi, "A hybrid-excited flux-switching machine for high-Speed dc-alternator applications," *IEEE Transactions on Industrial Electronics*, Vol. 61, No. 6, 2976–2989, 2014.
18. Hua, W., G. Zhang, and M. Cheng, "Flux-regulation theories and principles of hybrid-excited flux-switching machines," *IEEE Transactions on Industrial Electronics*, Vol. 62, No. 9, 5359–5369, 2015.
19. Liu, C., J. Zhong, and K. T. Chau, "A novel flux-controllable vernier permanent-magnet machine," *IEEE Transactions on Magnetics*, Vol. 47, No. 10, 4238–4241, 2011.
20. Zhu, X., L. Quan, D. Chen, M. Cheng, Z. Wang, and W. Li, "Design and analysis of a new flux memory doubly salient motor capable of online flux control," *IEEE Transactions on Magnetics*, Vol. 47, No. 10, 3220–3223, 2011.
21. Wang, Q., S. Niu, S. L. Ho, W. N. Fu, and S. Zuo, "Design and analysis of novel magnetic flux-modulated mnemonic machines," *IET Electric Power Applications*, Vol. 9, No. 7, 469–477, 2015.
22. Cheng, M., W. Hua, J. Zhang, and W. Zhao, "Overview of stator-permanent magnet brushless machines," *IEEE Transactions on Industrial Electronics*, Vol. 58, No. 11, 5087–5101, 2011.
23. Cheng, M., W. Hua, X. Zhu, W. Zhao, and H. Jia, "A simple method to improve the sinusoidal static characteristics of doubly-salient PM machine for brushless AC operation," *IEEE International Conference on Electrical Machines and Systems, ICMES*, 665–669, 2007.